Acta Biomaterialia 7 (2011) 2902–2909

Contents lists available at ScienceDirect

Acta Biomaterialia

journal homepage: www.elsevier.com/locate/actabiomat

Effect of surface modification on protein retention and cell proliferation under strain

J.P. Dunkers [a,*], H.-J. Lee [a], M.A. Matos [a,1], L.M. Pakstis [a,2], J.M. Taboas [b,3], S.D. Hudson [a], M.T. Cicerone [a]

[a] Polymers Division, National Institute of Standards and Technology, Gaithersburg, MD, USA
[b] Cartilage Biology and Orthopedics Branch, National Institute of Arthritis and Musculoskeletal and Skin Diseases, National Institutes of Health, Bethesda, MD, USA

ARTICLE INFO

Article history:
Received 25 August 2010
Received in revised form 29 March 2011
Accepted 7 April 2011
Available online 13 April 2011

Keywords:
Equibiaxial strain
Laminin
Polydimethylsiloxane
Smooth muscle cells
X-ray reflectivity

ABSTRACT

When culturing cells on flexible surfaces, it is important to consider extracellular matrix treatments that will remain on the surface under mechanical strain. Here we investigate differences in laminin deposited on oxidized polydimethylsiloxane (PDMS) with plasma treatment (plasma-only) vs. plasma and aminopropyltrimethoxysilane treatment (silane-linked). We use specular X-ray reflectivity (SXR), transmission electron microscopy (TEM), and immunofluorescence to probe the quantity and uniformity of laminin. The surface coverage of laminin is approximately 45% for the plasma-only and 50% for the silane-linked treatment as determined by SXR. TEM and immunofluorescence reveal additional islands of laminin aggregates on the plasma-only PDMS compared with the relatively smooth and uniform silane-linked laminin surface. We also examine laminin retention under strain and vascular smooth muscle cell viability and proliferation under static and strain conditions. Equibiaxial stretching of the PDMS surfaces shows greatly improved retention of the silane-linked laminin over plasma-only. There are significantly more cells on the silane-linked surface after 4 days of equibiaxial strain.

Published by Elsevier Ltd. on behalf of Acta Materialia Inc.

1. Introduction

Mechanotransduction is the process by which mechanical signals are transferred to cells from the surrounding environment via one of several pathways, such as the cytoskeleton or integrins [1,2]. This process is often studied by culturing cells on flexible substrates and applying strain [3]. Treatment of a flexible substrate, such as polydimethylsiloxane (PDMS), with extracellular matrix (ECM) proteins is necessary for successful cell adhesion, proliferation, and differentiation [4–6]. A concern is the ability of the protein to remain on the PDMS surface under physiological strains [7]. Therefore, it is important to develop methods to anchor the protein to the PDMS while maintaining its function.

Previous work focused on methods that promoted either physisorption, chemisorption, or covalent bonding between fibronectin or laminin and PDMS surfaces [8]. These surface treatments were examined in terms of protein amount, uniformity, roughness, and hydrophilicity. Also, the influence of these surface treatments on the attachment, proliferation, phenotype, and morphology of vascular smooth muscle cells (SMCs) was evaluated. Chemisorption methods, methods that promoted polar and hydrogen bonding interactions between ECM proteins and the PDMS surface, resulted in superior performance of the functionalized surface.

One particular chemisorption method resulted in the greatest protein amount and uniformity and highest SMC proliferation. This method involved the attachment of hydrolyzed aminopropyltrimethoxysilane (APTMS) to oxygen plasma-treated PDMS to provide an amine for polar interaction with the ECM proteins. Silane hydrolysis and grafting onto the oxidized PDMS surface occurred at 1 vol.% APTMS in ethanol at 70 °C. The present work extends this investigation to determine whether the more favorable physical properties of the aforementioned chemisorption method actually translate into improved SMC proliferation on laminin-coated PDMS compared with physically adsorbed laminin when subjected to mechanical strain.

Previous work demonstrated that identical proteins deposited on substrates with different physical and chemical properties do elicit different cell responses. For example, Kennedy et al. [9] fabricated surface energy gradients using a continuous variation in oxidation of a self-assembled monolayer of *n*-octyldimethylchlorosilane on glass and then deposited fibronectin. They discovered that the rate of cell proliferation was linearly dependent on surface energy and increased with increasing hydrophilicity. Also, the protein state plays an important role in its interaction with the surface. Brevig et al. [10] coated hydrophobic and relatively hydrophilic tissue culture polystyrene (TCPS) with native and denatured albumin. They found that the native albumin was adsorbed in different coverage amounts and topologies (aggregates

* Corresponding author. Tel.: +1 301 975 6841; fax: +1 301 975 4977.
E-mail address: joy.dunkers@nist.gov (J.P. Dunkers).
[1] Present address: Boeing Research and Technology, Seattle, WA 98108, USA.
[2] Present address: Synthes Inc., West Chester, PA 19380, USA.
[3] Present address: Department of Orthopedic Surgery, UPMC, Pittsburgh, PA 15260, USA.

1742-7061/$ - see front matter Published by Elsevier Ltd. on behalf of Acta Materialia Inc.
doi:10.1016/j.actbio.2011.04.005

vs. smooth surfaces), whereas the denatured albumin gave similar amounts and topologies. Rodriguez-Hernandez et al. [11] used atomic force microscopy (AFM) to probe laminin conformation on a series of co-polymers based on ethyl acrylate (EA) and hydroxyethyl acrylate (HEA) as a function of the co-polymer concentration. They showed that laminin presented a globular conformation at extremes of hydrophilicity (100 PHEA) and hydrophobility (100 PEA). At 50:50 by mass composition, laminin presented an extended conformation in the form of a network and the best neural cell proliferation and differentiation. These examples illustrate the dependence of cell response on the underlying substrate chemistry, even if separated by a protein layer.

Here we perform additional surface characterization on chemically and physically adsorbed laminin to elucidate physical differences in the protein layer using specular X-ray reflectivity (SXR), transmission electron microscopy (TEM), and immunofluorescence. SXR is a well-established technique used to characterize film thickness, average film density, and interfacial roughness of thin films and has a thickness resolution of the order of the wavelength of the X-ray radiation [12]. SXR analysis assumes continuous layers of uniform thickness and is not sensitive to islands of material on the surface if the fraction of those islands as a percentage of the total surface area is less than 20%. For proteins, SXR is used to elucidate thickness, coverage, and conformation on surfaces. Proteins have been adsorbed on ordered monolayers, such as Langmuir–Blodgett films or self-assembled monolayers, to drive specific interactions [13,14]. SXR is useful in obtaining surface concentrations using protein volume if a tertiary conformation can be assumed with confidence [15].

We performed further experiments to determine whether the physical differences of the laminin deposited using the two methods translated into differences in laminin retention and SMC proliferation under static and dynamic conditions. First, the robustness of the surface treatment was evaluated by monitoring the amount of laminin desorbed over time under static and equibiaxial strain conditions. We also cultured SMCs on various surfaces for 0 and 24 h in medium to demonstrate any enhancement of cell proliferation by the serum adhesion proteins under static conditions. We extended this concept to treated surfaces under equibiaxial strain to determine any differences in cell viability and proliferation.

2. Experimental

2.1. Preparation of PDMS surfaces

2.1.1. PDMS substrates

For static experiments, PDMS surfaces were made using Sylgard 184 PDMS (Dow Corning, Midland, MI) at a resin to crosslinker mass ratio of 10:1. The resin and base were hand mixed for 5 min and degassed under vacuum for 15 min. For the plate reader, Nikon microscope, and hemocytometry experiments, PDMS was cast into a 24-well plate with 0.2 ml in each well. The plate was degassed for an additional 15 min, placed on a level optical table, and cured for 48 h at 25 °C. For TEM and immunofluorescence using a confocal microscope, the PDMS was cast into a 1-well plate and cured.

2.1.2. PDMS film on silicon wafers

A 5% by mass solution of PDMS/base was dissolved in anhydrous heptane (Sigma–Aldrich, St Louis, MO) and filtered into a vial. Then, a 1 ml of solution was spun cast onto a silicon wafer (Silicon Quest International, Santa Clara, CA) at 210 rad s^{-1} for 90 s, after which it was annealed at 70 °C for 45 min to remove residual solvent.

2.1.3. PDMS oxidation via plasma treatment

All PDMS surface treatments were initiated with oxygen plasma according to published protocols [8]. Briefly, substrates were activated via oxygen plasma treatment using a Model SP100 Plasma Etcher (Anatach, Union City, CA) for 30 s at 30 W and an air flow rate of 20 sccm. Immediately following plasma treatment, silane or laminin solutions were applied to the substrates. The treatment protocols are described below.

2.2. Deposition of laminin

2.2.1. Physisorption

Mouse laminin (1.0 mg ml^{-1} in 50 mM Tris–HCl and 0.15 M NaCl at pH 7.4, Invitrogen, Carlsbad, CA) was physically adsorbed onto plasma-treated PDMS substrates (in well plates or on silicon wafers) via incubation at 10 μg ml^{-1} in distilled and deionized water for 18 h at 25 °C. In keeping with the protocol from our previous work [8], the buffered laminin solution was diluted 100× in distilled water to prepare the surface for dry analytical techniques used in the previous and current work. 100× dilution of the buffered laminin solution may lower the pH, but only minimally. Using this method, laminin was also adsorbed onto TCPS wells for comparison. PDMS surfaces prepared in this way on plasma-treated PDMS will be referred to throughout the paper as "plasma-only". Laminin surfaces prepared without plasma treatment will be referred to throughout the paper as "as-cured".

2.2.2. Chemisorption

Silane has commonly been employed for the attachment of proteins to silicone surfaces in the literature [16,17], and these PDMS substrates were prepared in a similar manner using aminopropyltrimethoxysilane [8]. Aminosilane on plasma-treated PDMS was verified using Fourier transform infrared attenuated total reflection (FTIR-ATR) spectroscopy by the presence of peaks at 1580 and 1500 cm^{-1} ($-NH_3^+$ deformation, results not shown). Substrates were incubated under ambient conditions as described above. Surfaces were again washed with distilled and deionized water to remove loosely bound protein. PDMS surfaces prepared in this way will be referred throughout the paper as "silane-linked".

2.3. Protein quantification and uniformity via immunochemistry

This procedure applies to all PDMS substrates used for both static and strain experiments. Prior to antibody attachment, the laminin surfaces were blocked with 1% bovine serum albumin (catalog No. A3059, Sigma–Aldrich, St. Louis, MO) in Dulbecco's 1× phosphate-buffered saline (PBS) (Gibco 14190, Invitrogen, Carlsbad, CA) for 20 min. Surfaces modified with laminin were labeled with the primary (1°) antibody rabbit anti-laminin (1:1000, Sigma–Aldrich) for 2 h at room temperature. After washing three times with PBS, the substrates were incubated for 2 h with Alexa Fluor 488 goat anti-rabbit IgG (1:100, Invitrogen) as the secondary (2°) antibody. Negative controls were performed with the following combinations of plasma treatmented PDMS: PDMS + 2°, PDMS + laminin + 2°, PDMS + 1° + 2°, PDMS + silane + 2°, PDMS + silane + laminin + 2°, and PDMS + silane + 1° + 2°. The fluorescence intensity from all controls was negligible.

The relative amount of protein on the PDMS substrate was measured using a Molecular Devices SpectraMax M5 plate reader at an excitation wavelength of 494 nm and an emission wavelength of 537 nm. Nine measurements per well were taken using five wells for each condition. Laminin was also imaged using a Zeiss LSM510 Confocal Microscope (LSCM) equipped with an argon ion laser for excitation at 488 nm and a 505–530 nm bandpass filter for emission. Images were collected using an air coupled, 20×, 0.4 numerical aperture long working distance objective. For all pro-

tein and cell measurements, error is expressed as one standard deviation. Analysis of variance was used for all data in this paper to determine significant differences with a 95% confidence interval.

2.4. Cell culture

Rat SMCs (A10) were purchased from ATCC (Manassas, VA) and maintained according to published protocols [18] in 5% CO_2 at 37 °C for both static and strain experiments.

2.5. Static cell adhesion and proliferation

Cells were seeded at a density of 5600 cells cm^{-2} (10,000 cells per well) in a 24-well assay plate containing the protein-modified PDMS substrates. After 5 h in culture, samples were visually checked to ensure cellular attachment, and all non-attached cells were removed from the well by gentle washing with PBS. These cells were counted via hemocytometry and used to calculate the number of cells that did not adhere to the surface. After 3 days in culture, the cells were detached from the substrates using trypsin/ethylene diamine tetraacetic acid (EDTA) and counted for total number. Cell proliferation was expressed as the total number of cells counted at 3 days minus the number of cells attached after 4 h. Cell counts for adhesion and proliferation were performed on six samples and are expressed using the average and one standard deviation.

2.6. Cell viability

For each well in a 6-well Bioflex (Flexcell International, Hillsborough, NC) culture dish, 1 ml of Dulbecco's modified Eagle's medium (DMEM), 0.5 μl of 4 mmol l^{-1} calcein AM and 1.5 μl of 2 mmol l^{-1} ethidium homodimer (Live/Dead Kit, Invitrogen, Carlsbad, CA) was added. The cells were incubated in medium with dye for 15 min and then rinsed once. Fresh growth medium was then added. The wells were then imaged under a Nikon Eclipse TE300 inverted microscope with a 4× objective using 530 nm excitation and 620 emission for the ethidium homodimer and 488 nm excitation and 520 nm emission for calcein AM.

2.7. Equibiaxial strain experiments

2.7.1. Laminin robustness under strain

The PDMS bottom of the Bioflex cell culture plates was oxidized and treated following either the plasma-only or silane-linked protocols, as described above. The Bioflex culture plates were used for both strain and static samples. Laminin was visualized using rabbit anti-laminin IgG (Sigma–Aldrich) and Alex Fluor 488 goat anti-rabbit IgG (Invitrogen). A detailed description of the equibiaxial strain system has been given by Chiang et al. [19]. To evaluate robustness, treated PDMS surfaces underwent continuous 5% equibiaxial strain at 0.5 Hz for 4 days. At 2 h, 1 day, and 4 days the strain was interrupted, samples were washed, and five microscope images were taken of each well, and the mean image intensity was normalized against the mean image intensity of 10^{-5} mol l^{-1} fluorescein in ethanol. The mean intensity was calculated from 25, 16-bit gray scale image histograms using the Image-Pro Plus (Media Cybernetics, Bethesda, MD) software. Error bars indicate one standard deviation.

2.7.2. Cell proliferation under equibiaxial strain

SMCs were seeded onto six laminin-modified Bioflex cell culture wells at 45,000 cells per well. The number of attached cells was counted after 4 h, after which the cells were further incubated for 12 h prior to straining. Another six wells were pre-conditioned with serum containing growth medium for 24 h prior to cell seeding. The wells were strained for 1 h at 5% peak equibiaxial strain and 0.5 Hz followed by static culture for 23 h. This cycle was performed twice, followed by continuous straining for 48 h, at which time the cells were detached using EDTA and counted. Cell proliferation was expressed as the total number of cells counted minus the number of cells attached. Error bars indicate one standard deviation.

2.8. Specular X-ray reflectivity

The SXR measurements were performed using a modified high resolution X-ray diffractometer in $\theta-2\theta$ configuration under specular conditions with the incident angle equal to the detector angle. A finely focused CuK_α X-ray source with a wavelength λ of 1.54 Å was conditioned with a four bounce Ge (2 2 0) monochromator and focused onto the film of interest. The detailed SXR measurements and data analysis were performed in a manner reported elsewhere [20]. In Table 1, the error in scattering length density (SLD) and layer thickness (d) are derived from the intrinsic error in the measurements and are Type B standard uncertainties. Errors in ρ_{eff} and Φ are computed using the error in the scattering length density and are Type B errors. A laminin density of 1.41 g cm^{-3} [21] and the atomic composition of phenylalanine were used to compute the surface coverage.

2.9. Transmission electron microscopy

The PDMS substrate was first coated with platinum/carbon by vacuum evaporation at an angle of approximately 14° to enhance surface topographic contrast. At this angle of evaporation, surface features cast shadows that are four times longer than their height. The sample was then coated with additional carbon at normal incidence. These evaporated films were then detached from the surface using a polyacrylic acid (PAA) technique. An aqueous solution of PAA (25% mass fraction) was deposited onto the surface and allowed to dry overnight at 55 °C. Afterwards, the dry glassy PAA was removed from the surface, detaching the thin films from the substrate. The adhesion of these films to the substrate was strong, however, and some cohesive failure of the PDMS also occurred. The resulting piece of PAA was placed on the surface of distilled water with the detached films on top. After dissolution of the PAA, the detached films were retrieved on copper grids and examined by TEM (EM400T, Phillips) operated at 120 keV in bright field mode using an objective aperture and slight underfocus.

3. Results and discussion

Laminins are a family of four-arm glycoproteins that interact with other proteins to form basement membranes. Laminin also self-assembles in the presence of Ca^{2+} ions to form a network and binds with cell integrins and non-integrin receptors believed to participate in mechanotransduction [22,23]. Investigation of

Table 1
Scattering length density (SLD), effective laminin density (ρ_{eff}), laminin coverage (Φ), and thickness (d) from SXR data fits.

PDMS treatment	SLD ($\times10^{-4}$) (±0.005 $Å^{-2}$)	ρ_{eff} (±0.011 g cm^{-3})	Φ (±0.01)	d (±1.0 nm)
As-cured (1)	2.18	0.479	0.34	3.0
As-cured (2)	1.80	0.395	0.28	5.6
Plasma-only (1)	2.81	0.617	0.43	2.0
Plasma-only (2)	3.01	0.661	0.47	4.3
Silane-linked (1)	3.43	0.754	0.53	2.2
Silane-linked (2)	3.29	0.723	0.51	4.4

the possible differences in laminin deposition between the two methods begins with a comparison of the amount on laminin on PDMS surfaces. We used conventional immunofluoresence to compare the laminin amount on as-cured PDMS, plasma-only PDMS, and silane-linked PDMS in Fig. 1 ($n = 45$). The asterisks show that, within the 95% confidence interval, the amount of laminin on the plasma-only and silane-linked PDMS is significantly greater than on the as-cured PDMS and TCPS. There is no significant difference in the amount of laminin between the as-cured PDMS and TCPS or between plasma-only and silane-linked treatments. We recognize that the ability to quantify the amount of laminin on the surface depends on the assumption that the polyclonal antibodies are binding in the same proportion to each laminin molecule. This may not be accurate, given the ability of the surface to affect protein conformation, as discussed earlier. Therefore, we looked at other techniques for comparison.

We conducted SXR measurements to quantify laminin coverage on PDMS using various treatments. To serve as a guide for fitting the critical angle, thickness, and roughness, SXR measurements were first performed on a single sample after each treatment step. A reflectivity scan was run on PDMS after curing, after plasma treatment, and after silane treatment (all samples without laminin). SXR data fits provided insights into the number of layers, layer density and thickness. Fig. 2 displays SLD profiles for the three treatment steps as a function of depth in the sample. For the as-cured PDMS, there is a ~50 Å thick top layer of material that is roughly 70% less dense than the underlying bulk layer. The plasma treatment then induces a densified layer about 100 Å thick. An approximately 10 Å thick silanized layer appears after the treatment with APTMS (silane-linked method). These critical angles, thicknesses, and roughnesses were used in fitting the multilayer systems with laminin.

Fig. 3 displays reflectivity curves for the as-cured PDMS with laminin, plasma-only PDMS with laminin, and silane-linked PDMS with laminin. From the guideline in the figure inset, we can see qualitatively that the as cured sample with laminin has the lowest critical angle (peak on the left of the guideline), which translates into the lowest laminin coverage. We can quantify the coverage by comparing the experimental protein layer density with the known density of the same or similar protein. Effective laminin coverage is calculated using the rule of mixtures after determining the laminin mass density using Eq. (1), where the experimental value for q_c^2 and constant r_0 are input to calculate ρ_{eff} (g cm^{-3}). ρ_{eff} is then normalized to the known protein density to obtain the protein coverage. For our work, we assume the density of laminin (850 kDa) to be 1.41 g cm^{-3}, as discussed previously [21]. This value is obtained from a master curve of theoretical protein density vs. relative molecular mass, where the function reaches an asymptote of 1.41 g cm^{-3} at 70 kDa. The experimental average density reported in that work is 1.37 g cm^{-3}. If a density of 1.3 g cm^{-3} is assumed then all surface coverage values are only 3% higher.

Table 1 displays the SLD, effective laminin density (ρ_{eff}), laminin coverage, and thickness for two samples each for the three conditions: as-cured, plasma-only, and silane-linked. Laminin coverage from X-ray reflectivity shows similar trends as for immunofluorescence. The amount of laminin on the as-cured PDMS is about 28–34%, while it is around 45–50% for both the plasma-only and silane-linked PDMS. The laminin coverage for the two samples prepared by the the silane-linked method is similar, given the error. The thickness (d) ranges from 2.0 to 4.4 nm for the

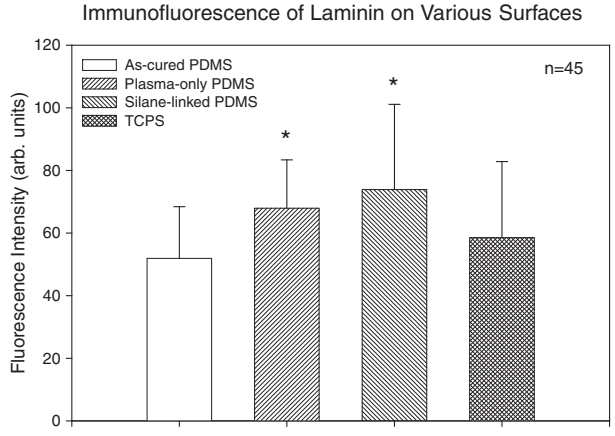

Fig. 1. Relative amounts of laminin on PDMS compared with TCPS measured by indirect labeling. Error bars indicate one standard deviation. Both plasma treatments resulted in significantly more laminin than on as-cured PDMS or on TCPS with $P < 0.05$. The amount of laminin on plasma-only vs. silane-linked PDMS is not significantly different.

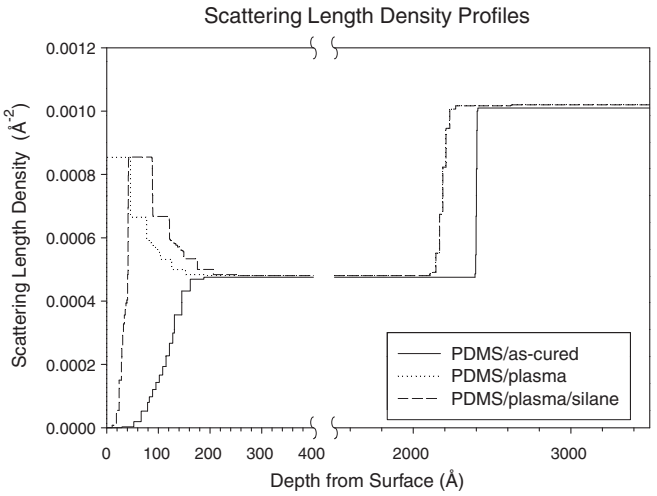

Fig. 2. SXR scattering length density reveals differences in surface layer density and thickness caused by plasma oxidation and subsequent silane treatment.

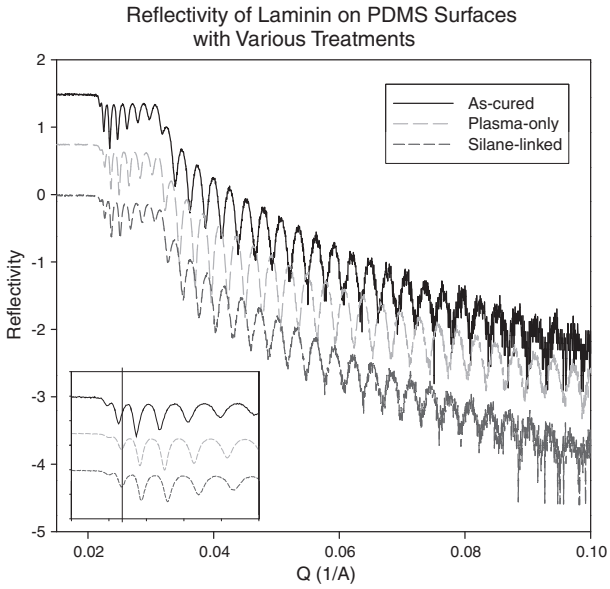

Fig. 3. SXR data collected from laminin adsorbed on as-cured PDMS, plasma-only PDMS with laminin, and silane-linked laminin on plasma-treated PDMS. A guideline in the inset indicates the critical angle of the as cured sample, which is proportional to the electron density of the layer. The as-cured sample with laminin has the lowest critical angle and qualitatively the lowest laminin coverage.

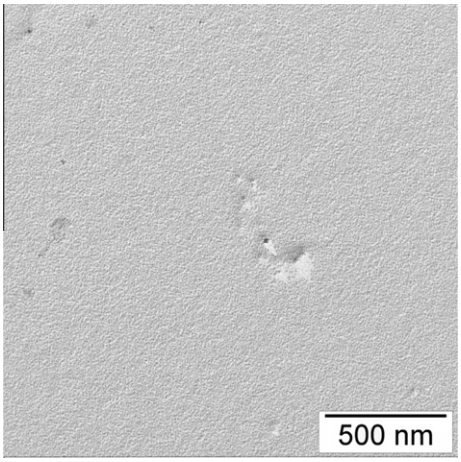

Fig. 4. TEM image of silane-linked treated PDMS.

plasma-only and silane-linked samples. The laminin coverage for the second sample of as-cured PDMS is substantially lower than the first, while the thickness of the laminin was substantially greater. The as-cured sample was included for comparison purposes, but not considered to be a useful treatment approach [7]. Therefore, it is not included in all analyses in this paper.

Since SXR averages the surface features over the measured area, TEM was performed to probe the uniformity of laminin deposition. Fig. 4 displays a TEM image of a laminin-free control surface that was treated by the silane-linked method. This surface is mostly smooth and featureless with occasional larger islands of material. TEM micrographs of plasma-only laminin treated surfaces are qualitatively different from the control surface in Fig. 4. Fig. 5 displays TEM micrographs at two different magnifications (Fig. 5A and B), where some laminin is manifested as irregularly shaped, light islands. The arrows show the direction of shadowing. In Fig. 5B, three representative protein aggregates from which height measurements were taken are circled. Enlarged features 2 and 3 are shown in insets. Feature 1 has a 150 nm step height, feature 2 has a 30 nm step height, and feature 3 has a 7.5 nm step height. Much of the laminin aggregate thickness is between the height of features 2 and 3, although there is an underlying roughness smaller in height than feature 3 that cannot be measured in these images stopped. For comparison, confocal fluorescence microscope images are displayed (Fig. 5C and D). The fluorescence signal is manifest as lighter gray areas, while black indicates regions of no signal. The confocal images corroborate the TEM images that indicate some laminin is deposited in patchy domains on the surface. It should again be noted that material that is less than 20% of the SXR sample area is not detected, as could be the case for the laminin aggregates.

Fig. 6 displays TEM (Fig. 6A and B) and confocal fluorescence (Fig. 6C) images of the silane-linked laminin. In contrast to Fig. 5, Fig. 6 shows several larger islands (Fig. 6A), but the laminin heterogeneity exists on a scale much smaller than in Fig. 5. The laminin surface appears to be much smoother even at a higher magnification (Fig. 6B). The confocal images in Fig. 6C and D reveal a much more uniform layer of laminin, as seen by the constant gray background of the image. The characterization results demonstrate that while both the plasma-only and silane-linked laminin surfaces have nominally the same level of monolayer coverage, the laminin on the plasma-only surface shows agglomeration not seen on the silane-linked surface.

The SXR, immunofluorescence, and TEM results together reveal differences in how the laminin is deposited onto the PDMS surface at different length scales. SXR has a sampling area of about 1 cm^2.

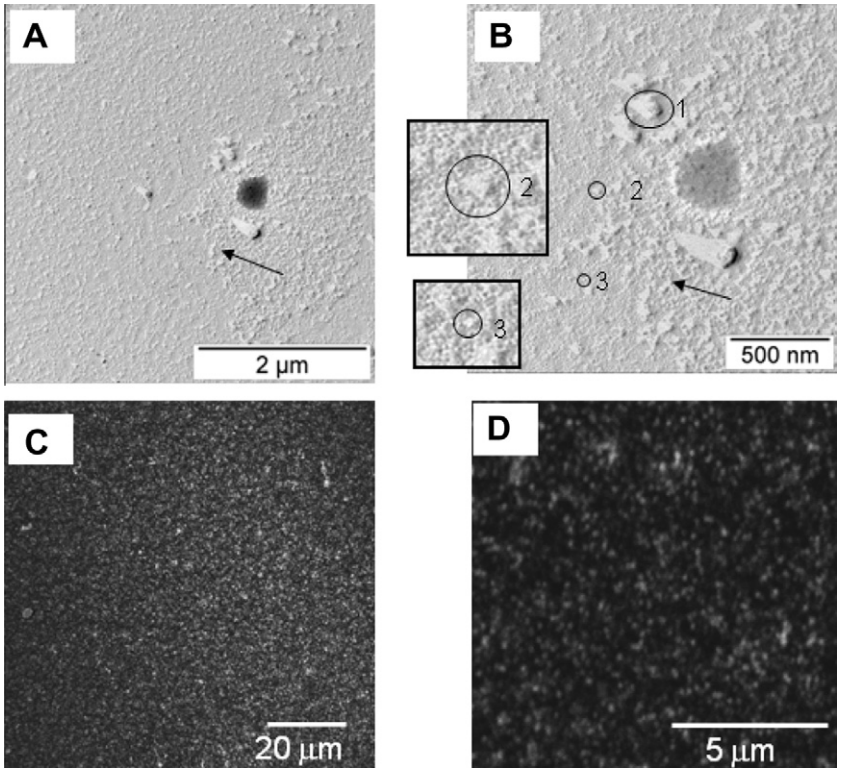

Fig. 5. Images of plasma-only PDMS with laminin. (A) Low magnification TEM with the arrow showing the direction of shadowing. (B) High magnification TEM with features marked for height measurement. Features 2 and 3 magnified in the insets. (C) Low and (D) high magnification immunofluorescence images. All images show the heterogeneous nature of laminin deposition.

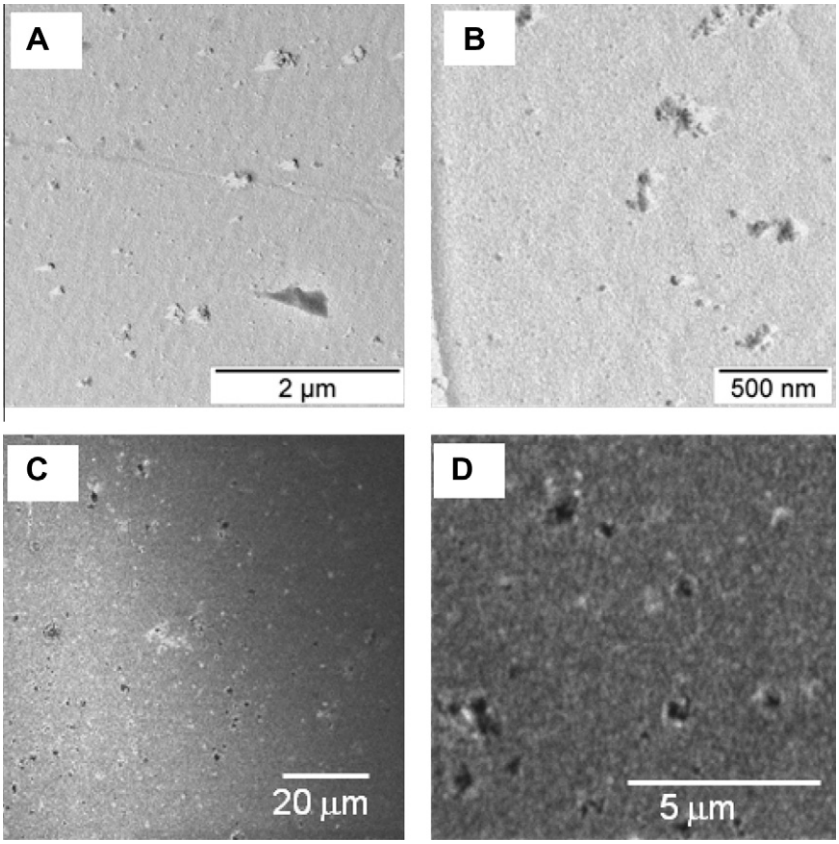

Fig. 6. Images of silane-linked laminin on PDMS. (A) Low and (B) high magnification TEM images. (C) Low and (D) high magnification immunofluorescence images. All images show mostly uniform laminin deposition with intermittent defects such as holes or islands relative to the plasma-only PDMS in Fig. 5.

The confocal immunofluorescence images can resolve down to several hundred nanometers, while this TEM captures features down to about 100 nm. The structure of laminin needs to be considered to understand these characterization results. Laminin has four arms. There are three short arms; two are about 34 nm in length while the third is about 48 nm [24]. The long arm is about 85 nm in length and consists of three chains oriented in a triple coiled-coil structure. Globular domains within the molecule dictate its thickness, and there is a 3 nm thick domain at the end of the triple coiled-coil long arm [22]. The SXR results, showing a thickness of around 3–4 nm, suggest that much of the laminin is lying flat on the surface for both surface treatment methods, given that this technique probes uniform films. The thin protein layer and low contrast between organic layers contributes to some measurement inaccuracy. The plasma-only and silane-linked laminin surfaces have approximately 45% and 52% coverage, respectively, although an insufficient number of samples were run to determine whether the small difference in coverage is significant. (The immunofluorescence results in Fig. 1 suggest that these coverages are not statistically different.) The amount of coverage makes sense given that the four-arm protein has been shown to polymerize into oligomers and higher order polymers through end to end association that are unable to densely pack [25]. In the TEM and fluorescence images, the silane-linked laminin appears as a mostly smooth, uniform surface. It has been shown that laminin will bind to myoblasts through the long arm terminal carboxylic acid group [26]. The plasma-only surface consisting primarily of polar hydroxyl groups does not promote as much laminin surface association as does the positively charged amine functionality. It is reasonable to assume that highly polar groups on laminin can form a strong electrostatic interaction with the amine, similar to the binding of amine to DNA on microarrays [27]. Interaction of laminin with the surface discourages strong self-association and globule formation. In fact, laminin aggregation on glass coverslips has been shown to occur when deposited at neutral pH [28]. The agglomerated laminin seen here is similar to that visualized by atomic force microscopy on hydrophobic surfaces [11] and is assumed to be weakly linked to the surface. However, the uniform surface of the silane-linked laminin does not necessarily translate into better retention over time or better cell adhesion during deformation. Therefore, we evaluated laminin retention and cell adhesion and proliferation under static, and equibiaxial strain conditions.

We hypothesized that the silane-linked surfaces would be able to retain more laminin than the plasma-only surfaces under mechanical deformation due to the strong polar interaction of the laminin with the amino-functional silane. Fig. 7 uses immunofluoresence to quantify the amount of laminin on a PDMS surface that has been treated as plasma-only or silane-linked. The treated PDMS surfaces formed the flexible bottoms of a 6-well Bioflex culture dish purchased without surface treatment. The treated Bioflex culture dishes were either static or underwent continuous equibiaxial stretching at 5% strain, 0.5 Hz for a total of 4 days (flex condition). Five immunofluorescence images were collected at random locations for each well, and five wells were sampled for each of the four conditions: plasma-only/static, plasma-only/flexed, silane-linked/static and silane-linked/flexed. The wells were gently washed three times with buffer before images were collected, and all image time points were collected sequentially on the same wells. Fig. 7 shows the amount of laminin as represented by the immunofluorescence intensity normalized to 0 h as a function of time where the asterisks denote a significant difference in the average from 0 h. After 4 days, the plasma-only/static sample re-

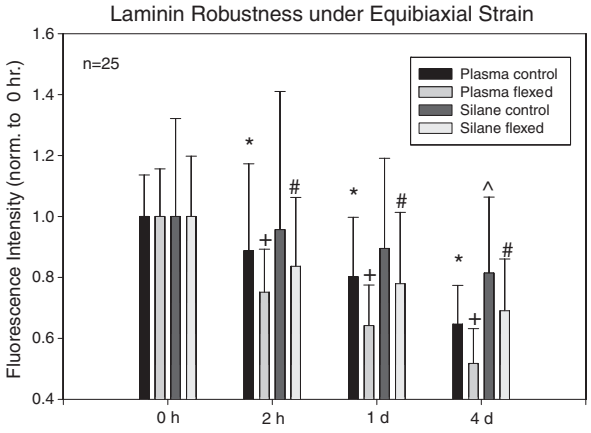

Fig. 7. Comparison of laminin retention on PDMS surfaces after plasma-only and silane-linked treatments under static and equibiaxial strain (flexed) conditions for up to 4 days as measured by indirect labeling. Error bars indicate one standard deviation. Symbols above a bar indicate intensities that are significantly different ($P < 0.05$) from 0 h.

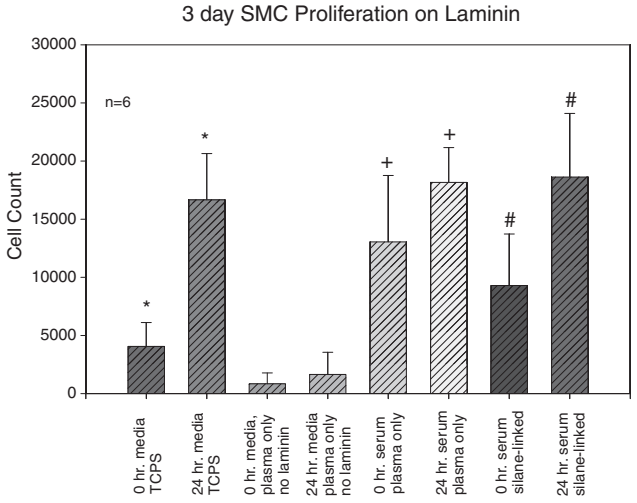

Fig. 8. Cell proliferation after 3 days under various conditions. Error bars indicate one standard deviation. Symbols above a condition pair indicate a significant difference between them ($P < 0.05$), except for the plasma-only pair ($P < 0.07$). 24 h serum incubation results in higher cell proliferation on TCPS (no laminin), plasma-only laminin and silane-linked laminin surfaces than 0 h incubation.

tains about 65% while the silane-linked static has about 80% of the starting amount of laminin. The plasma-only/static sample begins to show a statistically significant drop in fluorescence at the 1 day time point, which continues to 4 days, when the fluorescence intensity is about 50% of the initial level. The silane-linked/flexed sample retains 70% of the original amount of laminin at 4 days, which is significantly more than the plasma-only/flexed. In comparing the final amount of laminin on the surfaces, the silane-linked/static sample has significantly more than the silane-linked/flexed sample, which has significantly more than the plasma-only/flexed sample. The plasma-only/static sample has more than the plasma-only/flexed and less than the silane-linked/static samples.

The effect of laminin on SMC proliferation on the plasma-only and silane-linked surfaces under static conditions is shown in Fig. 8. A 24-well plate was incubated with serum for 0 or 24 h prior to seeding to reveal any additional effects serum adhesion proteins may have on cell proliferation that may mask the role of laminin. For the plasma-only and silane-linked laminin surfaces, the 24 h serum incubation resulted in statistically more cells than the 0 h serum incubation. The importance of serum adhesion proteins to cell proliferation has been demonstrated on TCPS, where cell proliferation after 24 h serum incubation is more than double that after no incubation. The number of cells was the same when comparing 24 h incubation of plasma-only with laminin, silane-linked with laminin and TCPS surfaces (no laminin). Cell proliferation was also compared between 0 and 24 h incubation without laminin. Both conditions led to cell counts of fewer than 5000, illustrating that serum proteins on an untreated PDMS surface were insufficient to promote cell proliferation. 24 h incubation enhanced the cell proliferation equally for TCPS, the plasma-only and silane-linked conditions.

Cell viability and proliferation under strain were examined. Cells were counted after undergoing 0.5% equibiaxial strain at 0.5 Hz. The strain cycle was 1 h strain and 23 h static for 2 days then continuous strain for another 2 days. Fig. 9 compares the cell proliferation for the plasma-only and silane-linked laminin substrates, for both 0 and 24 h serum incubation prior to seeding. The results show that the 24 h incubation advantage seen in Fig. 8 disappeared, most likely because the weakly bound serum proteins were dislodged by straining. There is no statistical difference in cell count for each treatment method between 0 and 24 h incubation. However, both silane-linked laminin treatments encouraged more cell growth than plasma-only laminin treatments. We hypothesize that the laminin shown in the characterization results could be loosely enough bound to be removed under strain. There were qualitatively more cells on the silane-linked laminin wells than the plasma-only wells, as seen by phase contrast images at 2 days (results not shown). The viability of SMCs was examined using live/dead staining (calcein AM/ethidium homodimer) to confirm the efficacy of the surface treatments. There were a negligible number of dead cells after 4 days for the static and strained plasma-only and silane-linked conditions (results not shown). The cells on both the plasma-only and silane-linked samples also showed a high degree of alignment after 4 days of strain (results not shown).

Laminin can anchor cells to the flexible PDMS surface through integrins and the non-integrin elastin/integrin receptor [23]. It can also indirectly tether the cells through its interaction with collagen produced by smooth muscle cells in the synthetic state. However, this work has shown it is the robust attachment of laminin to the PDMS substrate that dictates the ability of SMCs

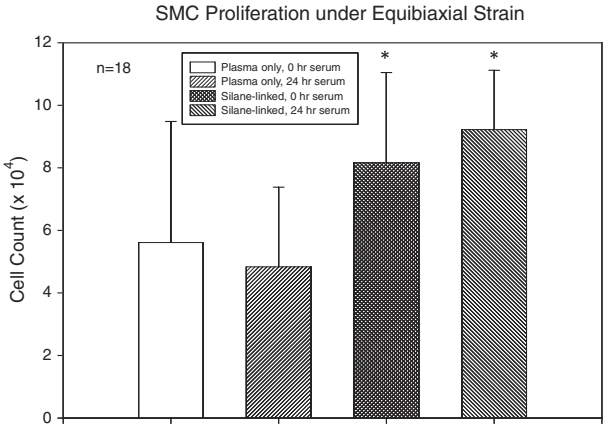

Fig. 9. Cell proliferation after 4 days under strain on plasma-only and silane-linked laminin surfaces after either 0 or 24 h serum preconditioning. 45,000 cells were seeded and attached for 12 h. Strain conditions: 0.5 Hz; 5% strain; 1 h strain, 23 h static for 2 days, then continuous strain for 2 days. Error bars indicate one standard deviation. Asterisks indicate that the cells on both silane-linked conditions are statistically indistinguishable and significantly more than the plasma-only condition ($P < 0.05$).

to remain attached during mechanical straining prior to confluency.

4. Conclusions

Laminin-coated PDMS substrates prepared using two different surface treatments were evaluated in terms of physical characterization of the laminin and the response of SMCs. One surface treatment was standard protein adsorption to the oxidized PDMS surface (plasma-only) while the other involved stronger polar interactions to an amino-functional silane attached to the PDMS substrate (silane-linked). Immunofluorescence and SXR shows comparable amounts of laminin on the plasma-only and silane-linked surfaces and statistically more laminin than on the as-cured PDMS and TCPS (immunofluoresence only). SXR shows a monolayer of laminin deposited on the surface for the plasma-only and silane-linked treatments. TEM reveals additional islands of laminin aggregates for the plasma-only PDMS treatment, while the silane-linked treatment exhibits a more smooth, featureless surface.

Static cultures of SMCs on laminin reveals increased cell proliferation after 24 h serum incubation on plasma-only PDMS, silane-linked PDMS, and TCPS surfaces when compared with 0 h incubation. Silane-linked treatment showed increased retention of laminin over the plasma-only treatment under strain, and the 24 h serum incubation advantage disappears. Under strain, the cells on the plasma-only surface proliferate to 50% of the number of cells on the silane-linked surface at 4 days.

This study has shown that depositing the laminin on a flexible surface with a tethered amino-functional silane provides a more uniform monolayer and improved retention under mechanical strain than standard physical adsorption. This improved laminin retention results in higher cell proliferation under strain.

Acknowledgements

The authors would like to acknowledge Khaled Aamer in the Biomaterials Group for his thoughtful review of the paper, Christopher Stafford for his technical assistance, and Stefan Leigh in the Statistical Engineering Division for his assistance with the statistical analysis.

This is an official contribution of the National Institute of Standards and Technology, not subject to copyright in the USA. Certain equipment, instruments or materials are identified in this paper in order to adequately specify the experimental details. Such identification does not imply recommendation by the National Institute of Standards and Technology nor does it imply the materials are necessarily the best available for the purpose.

References

[1] Huang H, Kamm RD, Lee RT. Cell mechanics and mechanotransduction: pathways, probes, and physiology. Am J Physiol Cell Physiol 2004;287(1): C1–C11.
[2] Wang JH, Thampatty BP. An introductory review of cell mechanobiology. Biomech Model Mechanobiol 2006;5(1):1–16.
[3] Kurpinski K, Park J, Thakar RG, Li S. Regulation of vascular smooth muscle cells and mesenchymal stem cells by mechanical strain. Mol Cell Biomech 2006;3(1):21–34.
[4] Hubschmid U, Leong-Morgenthaler PM, Basset-Dardare A, Ruault S, Frey P. In vitro growth of human urinary tract smooth muscle cells on laminin and collagen type I-coated membranes under static and dynamic conditions. Tissue Eng 2005;11(1/2):161–71.
[5] Ma Z, Mao Z, Gao C. Surface modification and property analysis of biomedical polymers used for tissue engineering. Colloids Surf B Biointerfaces 2007;60(2): 137–57.
[6] Toworfe GK, Composto RJ, Adams CS, Shapiro IM, Ducheyne P. Fibronectin adsorption on surface-activated poly(dimethylsiloxane) and its effect on cellular function. J Biomed Mater Res A 2004;71(3):449–61.
[7] Cunningham JJ, Nikolovski J, Linderman JJ, Mooney DJ. Quantification of fibronectin adsorption to silicone–rubber cell culture substrates. Biotechniques 2002;32(4):876. 878, 880.
[8] Pakstis LM, Dunkers JP, Zheng A, Vorburger TV, Quinn TP, Cicerone MT. Evaluation of polydimethylsiloxane modification methods for cell response. J Biomed Mater Res A 2010;92(2):604–14.
[9] Kennedy SB, Washburn NR, Simon Jr CG, Amis EJ. Combinatorial screen of the effect of surface energy on fibronectin-mediated osteoblast adhesion, spreading and proliferation. Biomaterials 2006;27(20):3817–24.
[10] Brevig T, Holst B, Ademovic Z, Rozlosnik N, Rohrmann JH, Larsen NB, et al. The recognition of adsorbed and denatured proteins of different topographies by beta2 integrins and effects on leukocyte adhesion and activation. Biomaterials 2005;26(16):3039–53.
[11] Rodriguez-Hernandez JC, Salmeron SM, Soria JM, Gomez Ribelles JL, Monleon PM. Substrate chemistry-dependent conformations of single laminin molecules on polymer surfaces are revealed by the phase signal of atomic force microscopy. Biophys J 2007;93(1):202–7.
[12] Lee HJ, Soles CL, Lin EK, Wu WL, Liu Y. Nonuniform structural degradation in porous organosilicate films exposed to plasma, etching, and ashing as characterized by X-ray porosimetry. Appl Phys Lett 2007;91 (17).
[13] Kusel A, Khattari Z, Schneggenburger PE, Banerjee A, Salditt T, Diederichsen U. Conformation and interaction of a D, L-alternating peptide with a bilayer membrane: X-ray reflectivity, CD, and FTIR spectroscopy. Chemphyschem 2007;8(16):2336–43.
[14] Petkova V, Benattar JJ, Nedyalkov M. How to control the molecular architecture of a monolayer of proteins supported by a lipid bilayer. Biophys J 2002;82(1 Pt 1):541–8.
[15] Evers F, Shokuie K, Paulus M, Sternemann C, Czeslik C, Tolan M. Exploring the interfacial structure of protein adsorbates and the kinetics of protein adsorption: an in situ high-energy X-ray reflectivity study. Langmuir 2008;24(18):10216–21.
[16] Altankov G, Grinnell F, Groth T. Studies on the biocompatibility of materials: fibroblast reorganization of substratum-bound fibronectin on surfaces varying in wettability. J Biomed Mater Res 1996;30(3):385–91.
[17] Lateef SS, Boateng S, Hartman TJ, Crot CA, Russell B, Hanley L. GRGDSP peptide-bound silicone membranes withstand mechanical flexing in vitro and display enhanced fibroblast adhesion. Biomaterials 2002;23(15):3159–68.
[18] Pauly RR, Bilato C, Cheng L, Monticone R, Crow MT. Vascular smooth muscle cell cultures. Methods Cell Biol 1997;52:133–54.
[19] Chiang MY, Cheng T, Pakstis L, Dunkers J. Solutions for determining equibiaxial substrate strain for dynamic cell culture. J Biomech 2010;43(13):2613–7.
[20] Wu WL, Wallace WE, Lin EK, Lynn GW, Glinka CJ, Ryan ET, et al. Properties of nanoporous silica thin films determined by high-resolution X-ray reflectivity and small-angle neutron scattering. Journal of Applied Physics 2000;87(3): 1193–200.
[21] Fischer H, Polikarpov I, Craievich AF. Average protein density is a molecular-weight-dependent function. Protein Sci 2004;13(10):2825–8.
[22] Engel J. Laminins and other strange proteins. Biochemistry 1992;31(44): 10643–51.
[23] Spofford CM, Chilian WM. The elastin–laminin receptor functions as a mechanotransducer in vascular smooth muscle. Am J Physiol Heart Circ Physiol 2001;280(3):H1354–60.
[24] Bruch M, Landwehr R, Engel J. Dissection of laminin by cathepsin G into its long-arm and short-arm structures and localization of regions involved in calcium dependent stabilization and self-association. Eur J Biochem 1989;185(2):271–9.
[25] Yurchenco PD, Cheng YS, Colognato H. Laminin forms an independent network in basement membranes. J Cell Biol 1992;117(5):1119–33.
[26] Colognato H, Winkelmann DA, Yurchenco PD. Laminin polymerization induces a receptor–cytoskeleton network. J Cell Biol 1999;145(3):619–31.
[27] Bowtell D, Sambrook J, editors. DNA Microarrays: A Molecular Cloning Manual. Cold Spring Harbor, NY: Cold Spring Harbor Press; 2003. p. 98.
[28] Freire E, Gomes FC, Linden R, Neto VM, Coelho-Sampaio T. Structure of laminin substrate modulates cellular signaling for neuritogenesis. J Cell Sci 2002;115(24):4867–76.